

Service Life Extension of Stainless Steel Wire Mesh Belts for Sintering Furnaces

Anna Wehr-Aukland and Donald J. Bowe,
Air Products and Chemicals, Inc.

Anthony M. Zaffuto and Jeremy Gabler,
Metaltech, Inc.



SERVICE LIFE EXTENSION OF STAINLESS STEEL WIRE MESH BELTS FOR SINTERING FURNACES

Anna Wehr-Aukland and Donald J. Bowe, Air Products and Chemicals, Inc.
Anthony M. Zaffuto and Jeremy Gabler, Metaltech, Inc.

ABSTRACT

The service life of stainless steel wire mesh belts in sintering furnaces is limited, because material deterioration results in wire fracture. A newly developed humidification system establishes a furnace atmosphere that maintains a protective oxide scale on the belt surface throughout the sintering process and at the same time creates an environment that is reducing to the sintered metal compact. This work includes thermodynamic calculations of the furnace atmosphere dew points that satisfy these oxidation / reduction criteria. Scanning Electron Microscopy, combined with Energy-dispersive X-ray Analysis, and mechanical testing methods have been used to compare belts that have undergone the same length of service in a nitrogen-hydrogen atmosphere and in an atmosphere that was modified using the newly developed humidification method. The material examinations have revealed that the new humidification system significantly extends the service life of stainless steel belts.

INTRODUCTION

Wire mesh belts are used to convey powder metal parts through continuous sintering furnaces. The most important aspect of mesh belt performance, which affects manufacturing costs and downtime, is service life. Different approaches have been investigated to extend service life of conveyor mesh belts, including material selection [1, 2], design-related factors, such as shape of the wire used to produce spiral loops [3] and modification of furnace atmosphere [4]. The alloy recommended by belt manufacturers as a cost-effective solution and commonly used for high temperature belt applications, such as copper brazing and powder metal sintering, is austenitic AISI Type 314 stainless steel (Table I).

Table I: Chemical Composition of Stainless Steel (weight %) [5]

Designation	C	Mn	P	S	Si	Cr	Ni
Type 314	0.25 max.	2.00 max.	0.045 max.	0.030 max.	1.50-3.00	23.0-26.0	19.0-22.0

Material degradation of a stainless steel belt during prolonged service in a sintering furnace is inevitable. The belt is nitrated by nitrogen from the nitrogen-based sintering atmosphere and carburized by carbon-bearing compounds that form during delubrication of powder metal parts. High temperature degradation phenomena involving creep, oxidation, carburization and nitridation are characteristic of austenitic stainless steels [6-8]. Carburization and nitridation lead to internal carbide and nitride precipitation, which may result in serious embrittlement [6-8]. Nitridation, carburization, deformation and abrasive wear are well recognized phenomena that contribute to wire mesh belt failure [1, 2, 4, 6]. Conveyor belts are taken out of service due to excessive cambering or rupture of spiral loops or cross-rods. In its final deterioration stage, the belt material becomes extremely brittle.

Stainless steels are protected from the corrosive effect of the environment, including carburization and nitridation, by a uniform surface layer of chromium oxide [6, 8]. However, in the high heat zone of a sintering furnace operating with a typical nitrogen-6% hydrogen atmosphere, the reducing environment destroys the protective chromium oxide scales. The belt is then re-oxidized as it passes through the lower temperature, more oxidizing cooling zone. Therefore, the belt is exposed to cyclic oxidation and reduction within the furnace. It has been observed that the service life of a stainless steel mesh belt can be extended by increasing the moisture content of a typical nitrogen-hydrogen sintering atmosphere [4]. The dew point of the atmosphere in the high heating zone of the furnace can be increased to maintain chromium oxide scales on the belt surface [4]. Moisture content that corresponds to the properly adjusted dew point does not result in decarburization of the parts being sintered [4].

In view of the described effects, this paper discusses the degradation of AISI Type 314 stainless steel belts exposed to two types of nitrogen-based atmospheres in a sintering furnace: a typical nitrogen-6% hydrogen gas mixture and a modified gas mixture of a similar composition. The modified furnace atmosphere was established using a newly developed cost effective humidification system. The atmosphere is modified to maintain a protective chromium oxide scale on the belt surface during the entire sintering process and at the same time prevent oxidation and decarburization of the sintered components.

PROCEDURE

Two wire mesh belts after 35 and 49 weeks of service in the same continuous sintering furnace were compared in this study. Both 12 inch wide belts with welded edges were made of AISI Type 314 stainless steel and were purchased from the same supplier. Chemical compositions of both belts are shown in Table II. The designation of the belts used in these study was BEF-36-10-8-10, which stands for balanced extra flat weave with 36 spiral loops per foot of width and 10 cross-rods per foot of length, 8 gauge rod and 10 gauge spiral.

Table II: Chemical Composition of belts B1 and B2 (weight %)

Belt	C	Mn	P	S	Si	Cr	Ni
B1 (Standard Atmosphere)	0.06	1.51	0.021	<0.001	2.10	23.2	18.6
B2 (Modified Atmosphere)	0.03	1.83	0.018	0.001	2.33	23.2	19.4

The industrial furnace employed in this evaluation was used for sintering parts pressed from various ferrous PM materials, including MPIF F-0000, F-0005, F-0008, FC-0205, FC-0208, and FN-0205, in a nitrogen-hydrogen atmosphere at 1129 °C (2065 °F), at the belt speed of about 99 mm/min (3.9 ipm).

These belts were pre-conditioned using the following conventional procedure, prior to using them for the sintering processes. During the pre-conditioning, the belts were heated in 55.6 °C (100 °F) increments per belt revolution under a nitrogen atmosphere (nitrogen flow was reduced by over 2 times as compared to the normal operating conditions). Each temperature was maintained for a period of 2 hours. At about 927° C (1700 °F), the furnace atmosphere was changed to the nitrogen – hydrogen based atmosphere corresponding to the long-term sintering experiment, which was different for each belt. Stepwise heating was continued until reaching the normal operating temperature of 1129 °C (2065 °F).

Two long-term sintering belt trials were carried out to test the belt in the presence of different nitrogen-hydrogen atmospheres. These atmospheres were introduced through an inlet port in the transition zone that was located between the high heating and cooling zones of the furnace. The first experiment was conducted using the standard nitrogen-hydrogen atmosphere containing 6% (by volume) hydrogen. Samples of the furnace atmosphere taken at different time intervals revealed that it contained less than 3 ppm oxygen and the dew point of the atmosphere in the high heating zone was -51°C (-60 °F). The second trial was carried out employing a newly developed humidification system. Analysis of the atmosphere in the high heating zone of the empty furnace revealed that the resulting atmosphere contained about 6.3 % hydrogen and 0.3% carbon monoxide. No carbon dioxide or methane was detected using an infrared tri-gas (CO, CO₂, and CH₄) analyzer. The dew point of the furnace

atmosphere was monitored by repeated analyses of the furnace atmosphere throughout this long-term sintering experiment. The dew point was maintained between -40 to -37 °C (-40 to -35 °F).

Samples from the belts used in the two trials were taken at 17, 31, 35 and 45 weeks of service. The material examinations performed on them included: microstructure analysis, tensile tests, microhardness tests and chemical composition (nitrogen and carbon concentrations) analysis. Microstructural analysis was conducted using optical microscopy (OM) and scanning electron microscopy combined with energy-dispersive X-ray microanalysis (SEM/EDX). SEM-EDX imaging was carried out using a JEOL 5910LV scanning electron microscope. The mounted cross-sections of belt wires and cross-rods were examined after applying a thin palladium-gold coating. Backscattered electron images and spectral maps were collected at either a 5 kV or 20 kV accelerating voltage. Metallographic samples for OM, SEM/EDX examinations and microhardness testing were prepared by mounting, grinding and polishing the spiral wires and cross-rods using standard practices. Tensile tests were conducted on cross-rods removed from the belt samples at 35 and 45 weeks of service in the sintering furnace following ASTM standards A370-10 and E8-09 [9, 10]. Confidence intervals at the 95% level were calculated for tensile strength, yield strength and elongation for at least 5 samples. Nitrogen and carbon concentrations of the spiral wires and cross-rods were determined using inert gas fusion / thermal-conductivity and combustion / infrared methods, respectively.

In addition to the examinations of the belts, the sintered parts were evaluated using standard quality control methods, including apparent hardness HRC tests and dimensional measurements. Statistical analysis was conducted on two part types made of MPIF FN-0205 material to investigate if the change from the standard to the modified atmosphere resulted in statistically significant differences in the apparent hardness and dimensions.

RESULTS AND DISCUSSION

Precipitation

OM and SEM examinations of the spiral wires and cross-rods from belt B1 operated in the standard furnace atmosphere and belt B2 after service in the modified atmosphere revealed precipitates on grain boundaries and within grains. These precipitates were not observed in the microstructure of the belt in the as-received condition. The concentration and size of large particles and the length of continuous chains of particles on grain boundaries increased with service time (Figure 1).

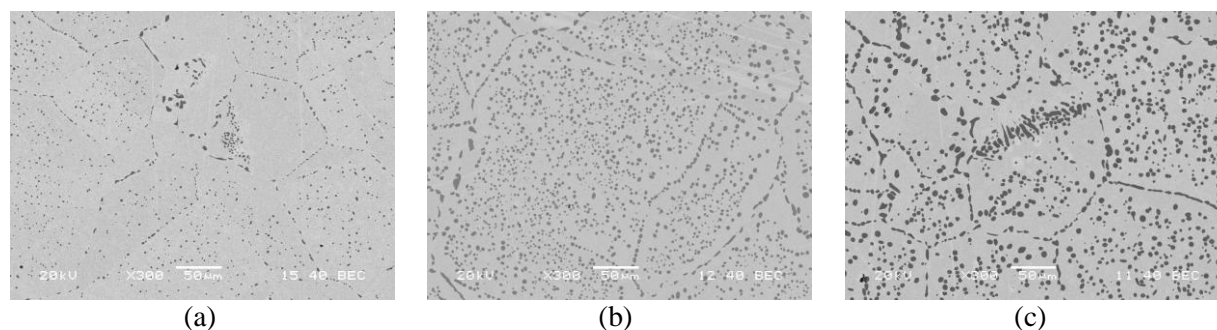


Figure 1. Representative microstructures of the central areas of the spiral wire B1 (standard atmosphere), transverse cross-sections, backscattered electron images (BEC): (a) 31 weeks in service; (b) 35 weeks in service; (c) 49 weeks in service.

Even though the precipitates were observed in the microstructures of both belts B1 and B2, the concentration and size of the particles, and the length of the continuous chains of particles in the cross-sections representing the same service times, were higher in the specimens from the standard atmosphere (Figure 2).

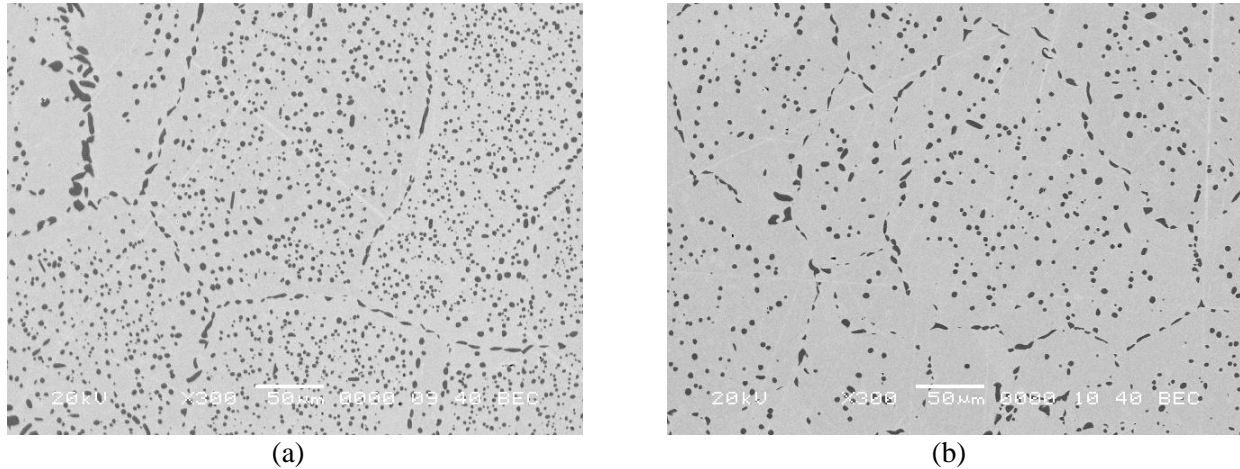


Figure 2. Central areas of the cross-rods after 35 weeks in service, transverse cross-sections, BEC: (a) belt B1 (standard atmosphere); (b) belt B2 (modified atmosphere).

SEM/EDX microanalysis revealed that the particles on grain boundaries and within grains consist of chromium and carbon, or chromium, carbon and nitrogen, or chromium and nitrogen, which indicates that they are chromium or chromium-rich carbides, carbonitrides, or nitrides. Examples of chromium or chromium-rich carbonitrides in the microstructure of belts B1 and B2 after 49 weeks of service are shown in Figures 3 and 4, respectively.

Increasing concentration and size of carbides, carbonitrides and nitrides with time is related to carburization and nitridation of the belt material during service in the sintering furnace. Higher concentration and size of the particles and the length of the continuous chains of particles on the grain boundaries in the microstructure of belt B1, as compared to the corresponding samples of belt B2, indicate that the deterioration of belt B1, which was exposed to the standard atmosphere, is more advanced.

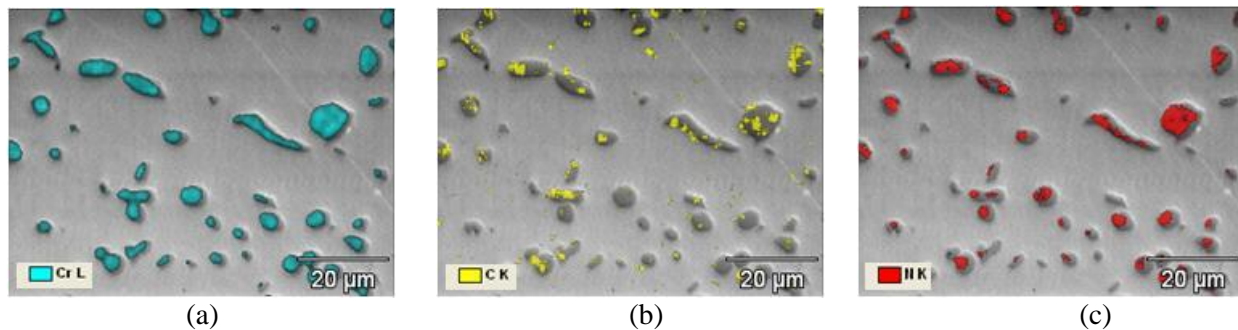


Figure 3. Transverse cross-section (central area) of the spiral wire from belt B1 after 49 weeks of service in the standard atmosphere, overlays of chromium (Cr), carbon (C) and nitrogen (N) on backscattered electron image, original magnification was 1500 times, accelerating voltage was 5 kV: (a) Cr (cyan); (b) C (yellow); (c) N (red).

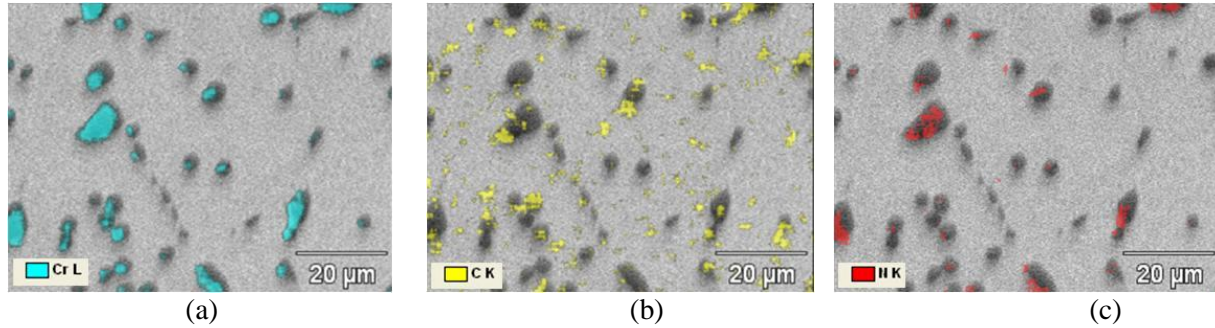


Figure 4. Transverse cross-section (central area) of the spiral wire from belt B2 after 49 weeks of service in the modified atmosphere, overlays of chromium (Cr), carbon (C) and nitrogen (N) on backscattered electron image, original magnification was 1500 times, accelerating voltage was 5 kV: (a) Cr (cyan); (b) C (yellow); (c) N (red).

Surface Oxide Scales, Chromium-depleted Zone and Internal Oxidation

SEM/EDX examinations of the oxide scales formed on the surface of the two belts (B1 and B2) during service in the sintering furnace revealed that the surface layers were composed of chromium and manganese-containing oxides. An example of the oxide scale on the belt after service in the standard atmosphere is shown in Figure 5. The oxide scale on belt B1 after 49 weeks of service in a standard atmosphere contained an iron-rich outer oxide layer (Figures 5f and 6a). The iron-rich outer oxide layer was not observed on the surface of belt B2 after service in the modified atmosphere (Figure 6b). An iron-rich oxide layer grows faster than the oxide that is rich in chromium [8]. Therefore, iron-rich oxide scales are not as protective as chromium-rich oxides.

On belt B2 after 35 weeks of service in the modified atmosphere, a virtually continuous silicon oxide layer was detected under the chromium-manganese oxide scale (Figure 6c). A silicon oxide layer can provide additional protection from the corrosive environment. A nearly continuous inner oxide layer may form at high oxidation temperatures at silicon concentrations of 1.5 to 2.5%, which is the case with AISI Type 314 steel [5, 6].

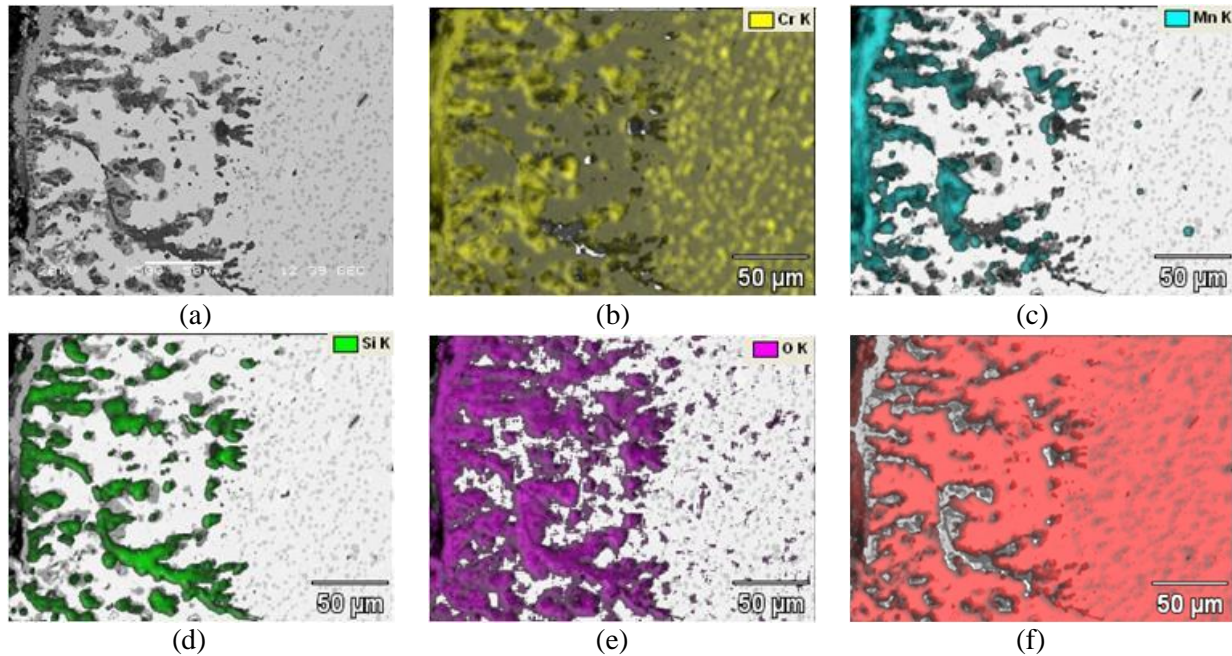


Figure 5. Surface and subsurface area of the spiral wire of belt B1 after 49 weeks in service, transverse cross-section, original magnification was 500 times, accelerating voltage was 20 kV: (a) backscattered electron image (BEC); (b) overlay of chromium on BEC; (c) overlay of manganese on BEC; (d) overlay of silicon on BEC; (e) overlay of oxygen on BEC; (f) overlay of iron on BEC.

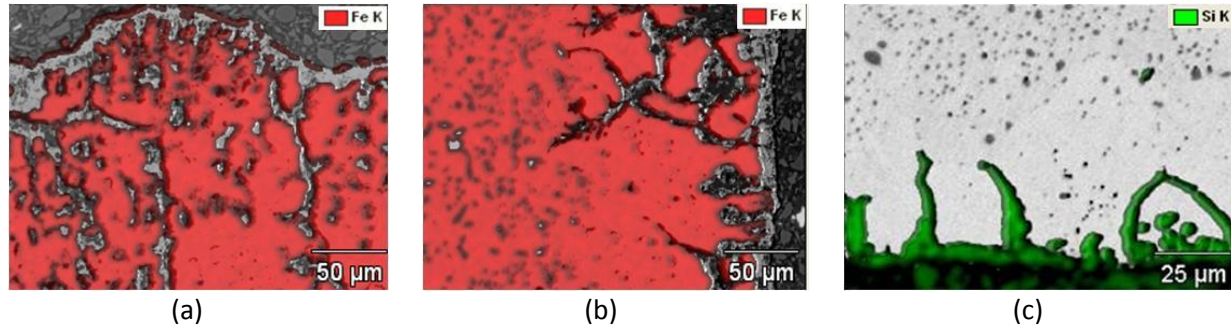


Figure 6. Surface and subsurface areas of spiral wires, transverse cross-sections, original magnification was 500 times, accelerating voltage was 20 kV, overlay of iron on BEC: (a) B1 after 49 weeks in service; (b) B2 after 49 weeks in service. Surface and subsurface area of a spiral wire from belt B2 after 35 weeks of service, original magnification was 1000 times, accelerating voltage was 5.0 kV, overlay of silicon on BEC (c).

Another degradation phenomenon involving thermal damage of both belts is internal oxidation. Under the continuous layer of chromium and manganese-containing surface oxide scales, areas of internal oxidation of chromium, manganese and silicon were observed. The internal oxidation depth is highest in the areas containing silicon oxide that was formed along grain boundaries. The internal oxidation depth is uniformly higher in belt B1, as compared to belt B2. Actually, the depth of internal oxidation of belt B2 was limited to 32 μm (1260 microinches) in 20 to 60% of the subsurface area, when measured on transverse cross-sections of the wires and cross-rods (Table III). Overall, the depth of internal oxidation for the samples of the belt after service in the modified atmosphere was about half that for the samples from the standard atmosphere.

Table III: Internal Oxidation Depth in Belts B1 and B2.

Furnace Atmosphere	Service Time (Weeks)	Rod Wire, μm (10^{-3} in.)		Spiral Wire, μm (10^{-3} in.)
		Prevalent	Maximum	
Standard	35	Prevalent	≤ 130 (5.12)	≤ 125 (4.92)
		Maximum	180 (7.09)	
Modified	35	Prevalent	< 25 (0.98)	≤ 50 (1.97)
		Maximum	110 (4.33)	
Standard	45	Prevalent	≤ 339 (13.35)	≤ 223 (8.78)
		Maximum	344 (13.54)	352 (13.86)
Modified	45	Prevalent	≤ 123 (4.84)	≤ 116 (4.57)
		Maximum	158 (6.22)	155 (6.10)
		Low Depth Area*	≤ 32 (1.26)	≤ 32 (1.26)

*Low depth area constituted 20 - 60% of the total subsurface area

Beneath the surface oxide scales, chromium carbide-denuded zones with no internal carbide formation (chromium-depleted zones) were observed in both belts B1 and B2. An example of the chromium-depleted zone is shown in Figure 7. Formation of this chromium-depleted region is caused by the consumption of chromium as the oxide is formed and dissolution of near-surface chromium carbides or carbonitrides [6]. Additional phenomena that damage oxide scale and increase consumption of chromium, such as oxide spallation and erosion [6], will affect the size of chromium-depleted zone. The chromium-depleted zone was considerably larger in belt B1 operated in the standard atmosphere, as compared to belt B2 after service in the modified atmosphere.

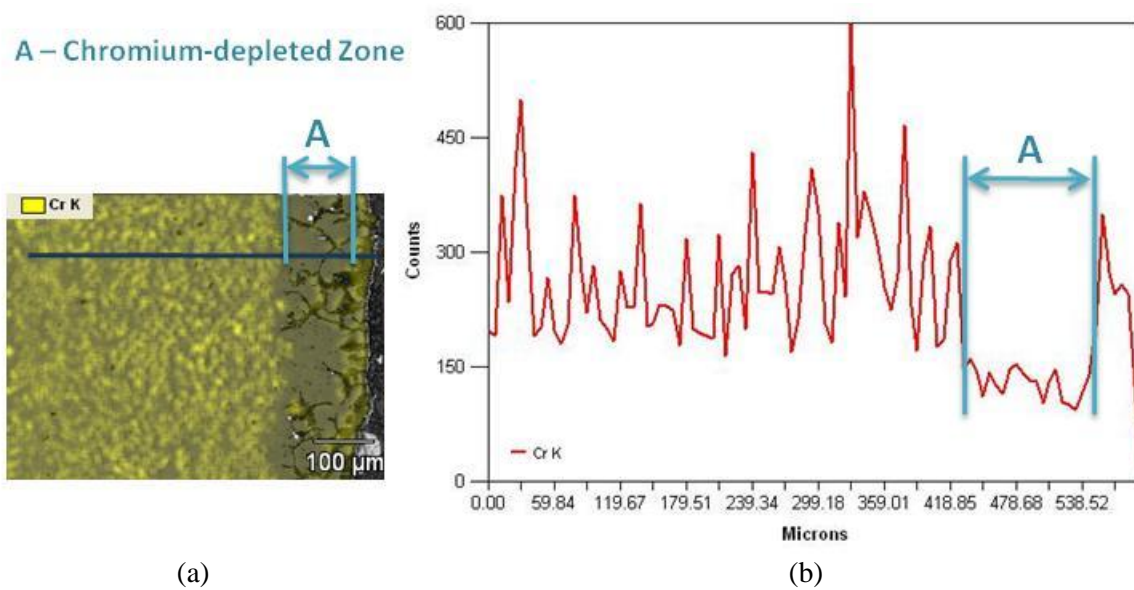


Figure 7. Chromium-depleted subsurface zone in a spiral wire from belt B2 after 49 weeks of service: (a) backscattered electron image with an overlay of chromium; (b) chromium distribution along the line shown in Figure 6(a).

In the subsurface regions of belts B1 operated in the standard atmosphere and belt B2 after service in the modified atmosphere, the extent of the chromium-depleted subsurface zone coincided with the depth of intergranular oxidation of silicon, or was higher in the areas of belt B2 where the material was well protected by the surface oxide scale. Two examples of chromium-depleted and internal oxidation zones are presented in Figure 8. Both examples show low-depth zones. However, “low-depth” has a relative meaning, depending on which of the two belts is considered. The difference between belts B1 and B2 is evident and substantial in respect to the width of the chromium-depleted and internal oxidation zone.

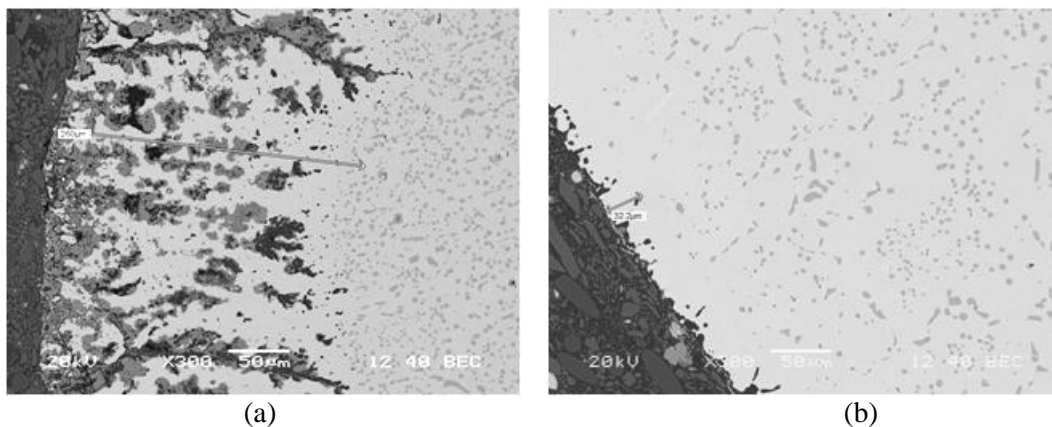


Figure 8. Low-depth subsurface oxidation of cross-rods from belts after 49 weeks in service, transverse cross-section: (a) belt B1 (standard atmosphere); (b) belt B2 (modified atmosphere).

Oxide scales on the surface of austenitic stainless steels are not fully protective from the high temperature corrosive environment [6-8]. If they were tight and well adherent, they would completely suppress carburization, because there is virtually no solid solubility of carbon in oxides [6]. However, all oxide scales, including Cr_2O_3 that is well recognized for its protective properties, contain pores and cracks [6]. Cracks are formed because of

creep, fatigue, or thermal cycling [6]. The effect of cracks depends on how fast they can heal, which is related to the rate of strain [6]. Conveyor belts need to be periodically shortened during their service life, because their length increases with time of service in a sintering furnace. Based on the microstructural analysis, cracks in the surface scale, related to load-affected deformation, creep and thermal cycling, seem to result in only minor intergranular oxidation in low-depth oxidation areas of belt B2 operated in the modified atmosphere (Figure 8b). However in some areas, the surface scale may experience additional mechanical damage, which results in more severe subsurface oxidation (for example the area shown in Figure 6b). This effect may be related to the severity of the oxide scale disruption and the furnace zone (temperature) where it occurs.

The dissimilarity in the range and uniformity of the subsurface oxidation can be explained by the difference in time when the protective scale was present at the surface of the belt. In the high heating zone of the furnace, belt B1 operated in the standard atmosphere was not protected by the chromium-rich oxide layer that would inhibit atomic transport necessary for selective internal oxidation to occur. The entire section of the belt was periodically exposed to the corrosive environment inside the sintering furnace. Even though the atmosphere was oxidizing to belt B2 inside the entire furnace, occasionally the protective oxide scale was mechanically disrupted, which resulted in increased internal oxidation in some areas of this belt. Nevertheless, even in the most severely attacked regions of belt B2, the internal oxidation depth was considerably lower than the oxidation depth in the subsurface area of belt B1 operated in the standard atmosphere.

The protective scale on belt B1 was repeatedly rebuilt when the reduced section of the belt moved to the oxidizing atmosphere of the cooling zone. This frequent reformation of the new surface scale consumed subsurface chromium. Furthermore, extensive oxidation of chromium in the subsurface region led to the increase in depth of the chromium-depleted zone of belt B1 operated in the standard atmosphere. These effects resulted in the higher depth of the chromium-depleted zone of belt B1, as compared to belt B2 operated in the modified atmosphere.

Chemical Composition

Chemical analysis of the belt materials after 35 and 49 weeks of service revealed that both materials absorbed carbon and nitrogen during service in the sintering furnace. The ingress of carbon into the belt materials was much smaller than the absorption of nitrogen. For example, in belt B2, the nitrogen content increased from the original 0.02% to the average of 0.93%, whereas carbon concentration increased from the original 0.03% to the average of 0.26% after 49 weeks of service. The major difference between belts B1 and B2 is not the carbon concentration, but the nitrogen content related to the amount of nitrogen absorbed by the belt material during service. The amounts of chromium-rich carbides, nitrides or carbonitrides on grain boundaries and within grains depend on the carbon and nitrogen contents of the material. The average combined carbon and nitrogen concentrations, presented in Figure 9, are higher for belt B1 operated in the standard temperature, which is in agreement with the observed higher concentration and size of precipitates in this belt material, as compared to the material of belt B2 after the same service times. In addition, the increase in the average combined carbon and nitrogen concentrations between 35 and 49 weeks in service was also higher for belt B1 after service in the standard atmosphere. The lower pickup of nitrogen by belt B2 operated in the modified atmosphere, as compared to belt B1 after the same time of service can be explained by protective properties of surface oxide scale on the surface of this belt. Most importantly, the protective chromium-rich oxide scale on the surface of belt B1 is destroyed in the reducing nitrogen-hydrogen atmosphere of the high heating zone exposing the surface to molecular nitrogen from the furnace atmosphere. Molecular nitrogen can be severely nitriding for austenitic stainless steels at the high temperatures that are characteristic of the high heating zone of a sintering furnace [7, 11].

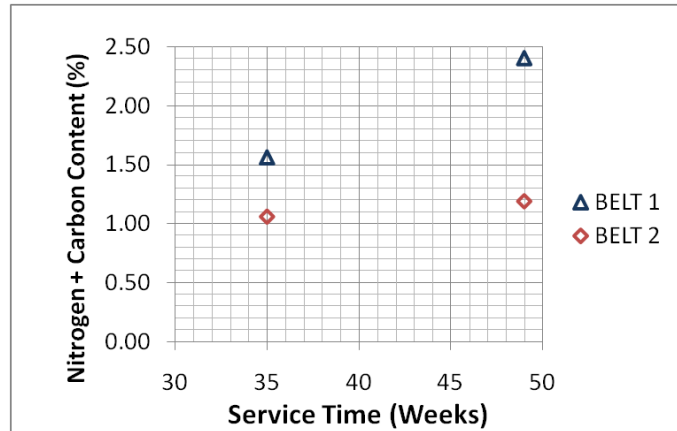


Figure 9. Average combined concentrations of carbon and nitrogen (in weight %) in belts B1 and B2.

Tensile Properties

Tensile properties of the cross-rods removed from belts B1 and B2 are shown in Figure 10. Average tensile strength, yield strength and elongation decrease with time in service. The reduction in tensile strength and elongation between 35 and 49 weeks of service was statistically significant for both belts. In addition, the average tensile strength, yield strength and elongation of the material of belt B2 operated in the modified atmosphere are higher, as compared to belt B1. Tensile strength of belt B2 is significantly higher than tensile strength of belt B1 after the same times of service. In addition, yield strength of belt B2 after 49 weeks in service is significantly higher than the yield strength of belt B1 after the same service time. The difference in elongation between the two belts after 35 weeks in service is also statistically significant (Figure 11).

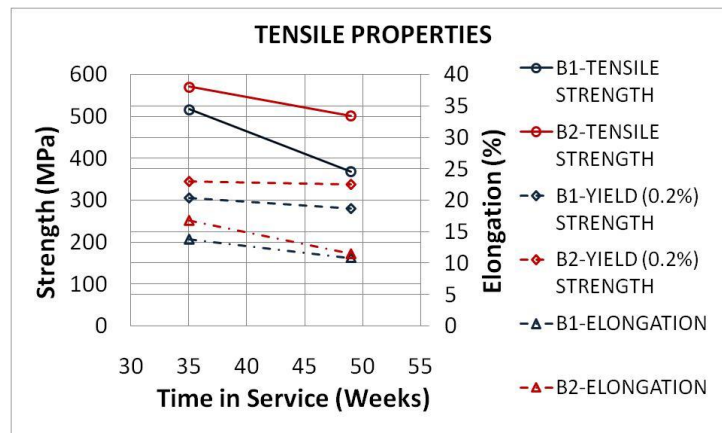


Figure 10. Tensile strength, yield strength and elongation of cross-rods removed from belts B1 and B2 after 35 and 49 weeks of service in a sintering furnace.

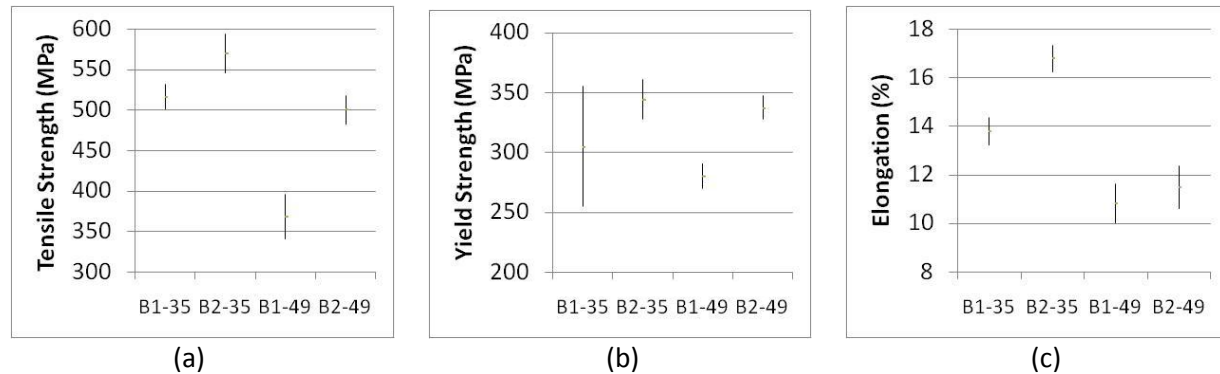


Figure 11. Tensile properties of cross-rods removed from belts B1 and B2; 95% confidence intervals for: (a) tensile strength; (b) yield strength; (c) elongation.

Carburization and nitridation-related precipitation of particles leads to loss of low temperature ductility and may affect the creep properties [6, 8]. Elongation is a measure of low temperature ductility. The tensile tests revealed that materials of both belts B1 and B2 become more brittle with time of service. Belt B1, as compared to B2, is significantly more brittle after 35 weeks of service. Even though the average elongation of the B2 cross-rods was higher than the corresponding value of belt B1, the difference in elongation is not statistically significant, which may be related to the low number of test samples. Nevertheless, cross-rods of belt B2 are significantly stronger after 49 weeks of service.

Carburization and nitridation may have only minor effect on tensile strength of stainless steels, as indicated by Grabke and Pillai [6, 8]. However, the tensile test results revealed that strength of the material decreased with time and was significantly lower for belt B1 operated in the standard atmosphere than for belt B2 after service in the modified atmosphere. These results suggest that the depth of the chromium-depleted zone which contains areas of internal oxidation, including intergranular oxidation, affects the strength of conveyor belts. Microhardness tests of the particle-containing regions and the chromium-depleted zones revealed that the microhardness of the latter was significantly lower, which indicates that the chromium-depleted zones have a lower strength. This indication, in combination with the larger size of the chromium-depleted zones of belt B1, may explain differences in strength of cross-rods from belts B1 and B2.

Assuming that the tensile strength is the main factor determining the service life of the belt and the tensile strength – time relationship is nearly linear between 35 and 49 weeks ($y = -10.597x + 887.3$), the material deterioration level of belt B2 after 49 weeks of service in the modified atmosphere (tensile strength of 500 MPa) corresponds to the deterioration level of belt B1 after only 36.5 weeks of service in the standard atmosphere. So, belt B2 needed an additional 12.5 weeks to reach the same level of deterioration as belt B1 after 36.5 weeks. Using 36.5 weeks as the reference point, the new atmosphere increased the service life of belt B2 by at least 34%.

Quality Control of Sintered Parts

Routine quality control tests and measurements have not revealed any problems related to the change from the standard to the modified furnace atmosphere. Additional statistical analysis conducted on two part types made of MPIF FN-0205 material did not detect any significant difference in the apparent hardness HRC and dimensions of the same type parts sintered in the standard and in the modified furnace atmospheres.

Thermodynamic Calculations

An oxidation-reduction diagram for the Fe-23Cr-19Ni system and pure iron under total pressure of 101325 Pa (1 atm) and partial pressure of hydrogen equal to 6079.5 Pa (0.06 atm), which corresponds to 6% (by volume) of hydrogen in the furnace atmosphere, is presented in Figure 12. The Fe-23Cr-19Ni system represents the main components of an austenitic AISI Type 314 stainless steel, and iron is the main component of MPIF F-0000,

F-0005, F-0008, FC-0205, FC-0208, and FN-0205 powder metal materials which were sintered in the stainless steel belt experiments conducted in this study. Addition of 2% Mn to the Fe-23Cr-19Ni system has virtually no effect on the location of oxidation-reduction curve in the temperature-dew point coordinates. The oxidation-reduction curves were calculated using FactSage™ software [12]. The diagram in Figure 12 shows that the dew point of -40 to -37 °C (-40 to -35 °F), which was maintained throughout the test in the modified atmosphere, was oxidizing to the stainless steel belt at the sintering temperature of 1129 °C (2065 °F) and at the same time was reducing to the sintered metal powder materials (point B in Figure 12). The position of point A in Figure 12 corresponds to the dew point and temperature of the standard furnace atmosphere in the high heating zone. The conditions indicated by point A are reducing to the austenitic stainless steel belt.

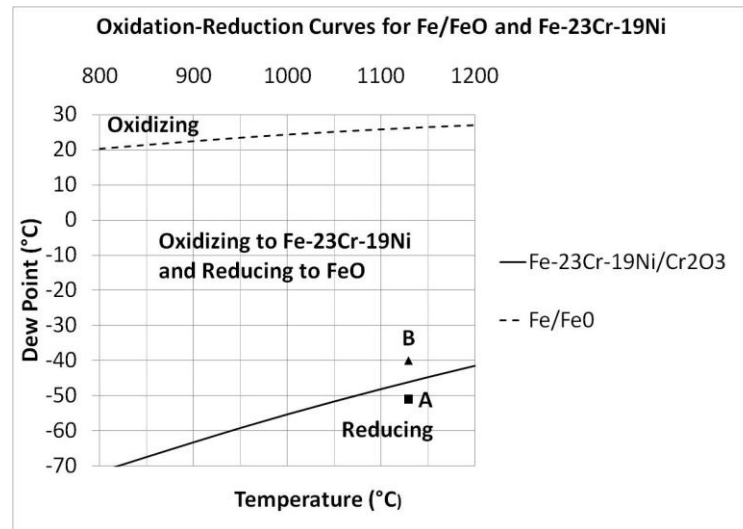


Figure 12. Oxidation-reduction diagram for Fe-23Cr-19Ni system and pure iron under partial pressure of hydrogen equal to 6079.5 Pa (0.06 atm).

CONCLUSIONS

The groundwork of this study was to compare degradation of two stainless steel wire mesh belts, one of which was exposed to a typical nitrogen-6% hydrogen atmosphere and the other to an atmosphere modified using a newly developed cost effective humidification system. It was found during this evaluation that the belt used in the humidified atmosphere was better protected from the adverse effects of corrosive environment, such as oxidation, nitridation and carburization, than the belt operated in a standard nitrogen-6% hydrogen gas mixture. This superior protection is attributed not only to the continuous presence of the oxide scales on the belt surface, but also to better properties of the surface oxide layer. Improved protection resulted in a lower rate of nitridation, which delayed embrittlement, as well as decreased rate of chromium depletion and reduced internal oxidation, which postponed loss of strength. Overall, the depth of internal oxidation for the samples of the belt B2 after service in the modified atmosphere was about half that for the samples from the standard atmosphere.

The superior protection of the belt B2 operated in the modified atmosphere affected the concentration and size of the particles and the length of the continuous chains of the particles on grain boundaries (carbonitrides and nitrides) and delayed the material deterioration. Higher concentration and size of the particles and the length of the continuous chains of particles on the grain boundaries in the microstructure of belt B1, as compared to the corresponding samples of belt B2, indicate that the deterioration of belt B1, which was exposed to the standard atmosphere, is more advanced. Assuming that the tensile strength is the main factor determining the service life of the belt and using 36.5 weeks as the reference point, the new atmosphere increased the service life of belt by at least 34%. The newly developed humidification system reduces the rate of service-related material deterioration and thus extends service life of stainless steel wire mesh belts.

ACKNOWLEDGEMENTS

The authors are grateful to Mr. James Stets for assistance in SEM/EDX analysis and Mr. John L. Green for help with sample preparation and on-site equipment installation.

This paper was first presented at PowderMet 2011 and was published in the conference proceedings.

REFERENCES

1. G.D. Smith and R.A. Smith, "Characteristics of Current and Advanced Wire Mesh Belt Alloys for Sintering Furnaces", *Industrial Heating*, October 1995, pp. 61-63.
2. G.D. Smith, H.L. Flower and R.D. Riva, "Alloy Selection Criteria for High Temperature Sintering Belts", *Advances in Powder Metallurgy & Particulate Materials*, compiled by C.L. Rose and M.H. Thibodeau, Metal Powder Industries Federation, Princeton, NJ, 1999, part 3, pp. 17-28.
3. M.F. Coyle and R.D. Riva, "Finite Element Analyses of Wire Mesh Furnace Belts", *Advances in Powder Metallurgy & Particulate Materials*, compiled by H. Ferguson and D.T. Whychell, Metal Powder Industries Federation, Princeton, NJ, 1999, part 1, pp. 83-93.
4. J.G. Marsden, D.J. Bowe, K.R. Berger and D. Garg, D.L. Mitchell, "Atmospheres for Extending Life of Belts within Sintering Furnaces", U.S. Patent No. 5,613,185, March 18, 1997.
5. Passport to Steel powered by CASTI, ASTM International, <http://www.casti.ca/database/>
6. H. J. Grabke, *Carburization – A High Temperature Corrosion Phenomenon*, MTI publication no. 52, 1998, Material Technology Institute of the Chemical Process Industries, St. Louis, MO.
7. G. Y. Lai, *High Temperature Corrosion and Materials Applications*, 2007, ASM International, Materials Park, OH.
8. S. R. Pillai, "High Temperature Corrosion of Austenitic Stainless Steels", *Corrosion of Austenitic Stainless Steels: Mechanism, Mitigation and Monitoring*", edited by H.S. Khatak and B. Raj, Woodhead Pub., Cambridge, UK, Alpha Science, Pangbourne, UK, 2002, pp. 265-286.
9. ASTM A370-10, Standard Test Methods and Definitions for Mechanical Testing of Steel Products.
10. ASTM E8-09, Standard Test Methods for Tension Testing of Metallic Materials.
11. R.H. Shay, T.L. Ellison and K.R. Berger, "Control of Nitrogen Absorption and Surface Oxidation of Austenitic Stainless Steels in H₂-N₂ Atmospheres", 1983, Air Products Technical Data, Air Products and Chemicals, Inc., Allentown, PA.
12. FactSage™ thermochemical software and database package developed jointly between Thermfact/CRCT (Montreal, Canada) and GTT-Technologies (Aachen, Germany), version 6.2, 2010.

For more information,
please contact us at:

**North America,
Corporate Headquarters
Air Products and Chemicals, Inc.**
7201 Hamilton Boulevard
Allentown, PA 18195
Tel 800-654-4567 or 610-706-4730
Fax 800-272-4449
Email gigmrktg@airproducts.com

**Asia
Air Products Asia Inc.**
1001, 10/F, Sunning Plaza
10 Hysan Avenue, Causeway Bay Hong
Kong
Tel 852-2527-1922
Fax 852-2527-1827
Email infoasia@airproducts.com

**Europe
Air Products PLC**
Hersham Place
Molesey Road
Walton-on-Thames
Surrey KT12 4RZ - UK
Tel +44 (0)1270 614314
Email apbulkuk@airproducts.com



tell me more
www.airproducts.com/mp